Anisotropic Stiffness Tensor Measurement for Standing Trees using Acoustics

Mathew Legg and Stuart Bradley

Department of Physics, University of Auckland
Auckland, New Zealand
e-mail: m.legg@auckland.ac.nz and s.bradley@auckland.ac.nz

ABSTRACT

Acoustic non-destructive testing techniques have been developed to measure properties, such as stiffness, of standing trees and logs. Standing tree stiffness measurements are commonly calculated by inserting two probes into the "same face" of the tree stem, hitting one with a hammer, and measuring the propagation time of the resulting acoustic signal between two probes. Studies have suggested that these time of flight measurements are biased to measure the outerwood stiffness rather than that of the tree stem as a whole and may vary between different hammer hit strengths and hence between users. In this paper, we explore a multipath acoustic technique for measuring components of the anisotropic stiffness matrix of tree stems, which describes the mechanical properties of wood. This technique uses anisotropic acoustic wave propagation velocity measurements made along the surface and through a standing tree. This technique was used to calculate an average stiffness through the tree's cross-section. Different acoustic/ultrasonic excitation techniques are investigated which obtain velocity measurements that are independent of the user.

INTRODUCTION

The stiffness of wood is related to the Modulus of Elasticity (MOE), or Young's E modulus, of the wood. Bending tests can be used to measure the static modulus of elasticity. However, these are generally destructive tests. Acoustic nondestructive testing (NDT) techniques have, therefore, been developed to measure the dynamic modulus of elasticity *E*. This is calculated using

$$E = \rho c^2 \tag{1}$$

where c is the acoustic wave velocity in the longitudinal direction, see Figure 1, and ρ is the mass density of material (Ross and Pellerin, 1994). For logs, the velocity is usually measured using acoustic resonance. The end of the log is hit with a hammer and the signal is recorded and the spectrum obtained. The resonance acoustic velocity is then calculated for the n^{th} resonance frequency f_n using

$$c_{RES} = \frac{2Lf_n}{n}, \tag{2}$$

where *L* was the length of the log. Resonance techniques have been reported to give stiffness measurements that compare well with static MOE values obtained using bending tests (Harris, Petherick and Andrews, 2002). Different resonance harmonics may generate different results. According to Chauhan and Walker (2006), the second harmonic appears to be that used by the commercial resonance tool Hitman[1].

Resonance cannot be used for standing trees. Instead the stiffness is measured using TOF techniques (Wang et al., 2001). These measurements are generally obtained by inserting two probes into a tree stem on the "same face" of the tree, separated vertically by a distance *z*, usually about a meter, see Figure 2(a). The acoustic velocity is calculated from the acoustic propagation time *T* between the two probes using

$$c_{TOF} = \frac{z}{T}, \tag{3}$$

The TOF is measured by detecting the start time of the signal. TOF measurements are reported to be noisier than resonance measurements. Some have reported that TOF measurements can vary with hammer hit strength. TOF techniques have also been reported to provide stiffness measurements that are higher than those obtained using resonance or bending tests (Wang, Ross and Carter, 2007). This has been suggested to be due to the increase in stiffness and hence acoustic velocity in tree stems from pith to bark (Hsu, 2003; Wang et al., 2004; Chauhan and

[1] http://www.fibre-gen.com

Walker, 2006; Lasserre, Mason and Watt, 2007). An alternative explanation is that the TOF method measures a "dilation speed", while the resonance measures the "rod speed" (Andrews, 2002; Wang, 2013).

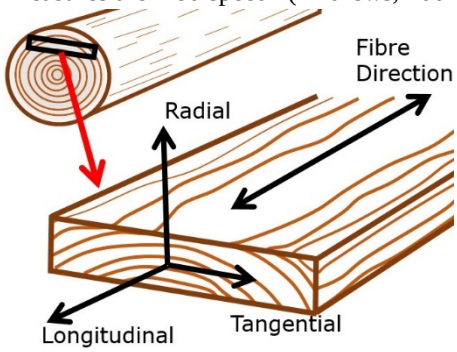

Figure 1: **Diagram illustrating the longitudinal, radial, and tangential orthotropic axis directions for wood.**

There have been results which suggest that "same face" TOF stiffness measurements are more closely correlated to with outerwood stiffness (Grabianowski, Manley and Walker, 2006; Mora et al., 2009). To try to compensate for this, some studies have made TOF measurements on "opposite faces" of the tree with the probes separated vertically by about a meter, see Figure 2(b) (Joe et al., 2004; Mahon et al., 2009; Matheson et al., 2002; Dickson, Raymond, Joe and Wilkinson, 2003; Dickson et al., 2004; Mahon, 2007). However, none of these studies have allowed for the anisotropic nature of wood, where the velocity in the radial direction is significantly less than that in the longitudinal direction. This resulted in stiffness measurements that were too low. Also, most have not included the true propagation path distance in the TOF velocity measurements, which has resulted in stiffness measurements that varied with the diameter of the tree stem. This means that the longitudinal velocity cannot be calculated using Equation (3).

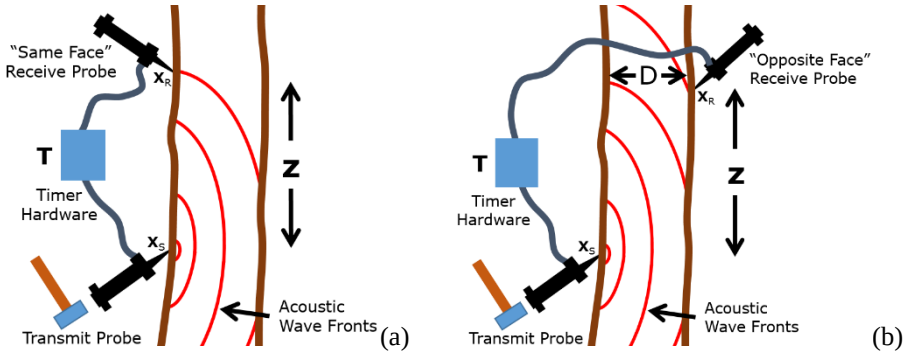

Figure 2: **Diagrams illustrating time of flight velocity measurements made using (a) "same face" and (b) "opposite face" techniques.**

In order for the "opposite face" method to be used for longitudinal velocity measurements, a model of the anisotropic wave propagation in tree stems needs to be obtained for the longitudinal-radial plane. Acoustic TOF measurements in logs have been presented in references (Zhang, Wang and Su, 2011; Zhang, Wang and Ross, 2009; Su, Zhang and Wang, 2009), though wave propagation models were not provided. Searles (2012) analyzed the data provided by Zhang, Wang and Su (2011) and suggested the wave fronts in the longitudinal-radial plane could be explained by elliptical velocities with the ellipse axes being the longitudinal and radial velocities. Anisotropic wave propagation models in the radial-tangential plane have been investigated in references (Dikrallah et al., 2006; Maurer et al., 2006; Li et al., 2014) for 2D tomography corrections. Maurer et al. (2006) provided a model which was a first order approximation of an ellipse. A 3D anisotropic model may be derived from Kelvin-Christoffel equation (Carcione, 2007a; Bucur, 2006). However, papers verifying this model experimentally for tree stems were not found in the literature.

In this paper, “same face” and “opposite face” techniques are investigated using multi-path TOF measurements for standing trees. The “opposite face” data are analyzed and a propagation model is presented, which attempts to fit the measurements for this tree. This model includes the anisotropic nature of wave propagation in wood and the propagation distance. The effect of using different hammer hit strengths is investigated. Longitudinal acoustic velocity values obtained using this techniques are compared the “same face” technique.

EXPERIMENTAL PROCEDURE

Measurements were made in this study using a standing radiata pine tree, which was located on private land at Hamurana near Rotorua. This had a DBH of 509 mm. Hitman ST300 test will be performed shortly on this tree. It is planned that this tree stem will also be cut down and resonance acoustic velocity tests performed. A range of measurements were performed on this tree stem using different excitation methods. This paper will describe measurements made using “same face” and “opposite face” methods for hammer hit excitation and an array of transducers, see Figure 3.

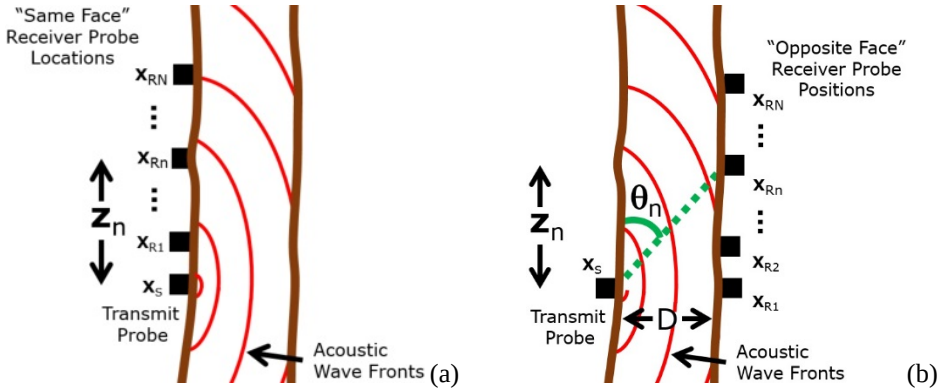

Figure 3: **Diagrams show (a) “same face” and (b) “opposite face” measurement setup for standing trees.**

Figure 4 shows the experimental setup used for this work. Twelve shear PZT transducers were attached vertically up one side of the tree stem with a separation of about 100 mm. This was achieved by screwing steel plates onto the tree stem and using a transducer holder composed of magnets and springs. The wood screw and steel plate provide acoustic coupling of the transducer to the tree stem through the bark. No preamplifiers were used for this work. This was done so that the signal amplitude would ideally be proportional to the hammer hit strength. The transducers were connected to ADC hardware capable of sampling all channels simultaneously at a sampling rate of 750 kHz and a resolution of 16 bits. Data acquisition software written in Matlab was used to capture the signal from the transducer array. The excitation source used was hammer hits on a 120 mm long flat head nail driven into the stem near the lower transducer on either the “same face” or “opposite face” relative to the transducers.


(a) (b)

Figure 4: Photo (a) shows an array of transducers attached to a tree stem for measurement of same face and opposite face measurements. Photo (b) shows a close up of one of the transducers.

PROCESSING HAMMER HIT DATA

Figure 5 shows two example plots obtained using two different hammer hit strengths. No preamplifiers were used for these measurements. While this resulted in more noisy TOF measurements, this was done to prevent the measured signals from clipping. This allowed the relative strengths of different hammer hits to be estimated from the signal amplitude. An alternative technique could have been to have one of the transducers (reference transducer) with no preamp while the rest had preamps. The reference transducer could then have been used to estimate relative hammer hit strength while the rest could be used for TOF measurement. This method would be expected to have resulted in lower noise. Hopefully these measurements will be made in the future.

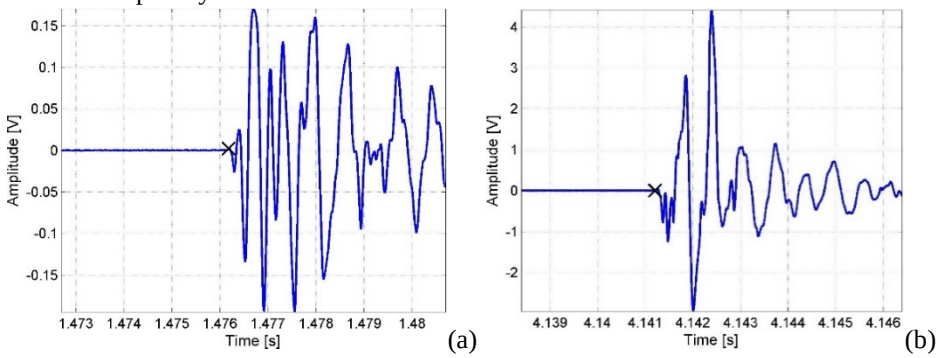

Figure 5: Example acoustic signals measured on a transducer attached to a tree stem resulting from hammer hits on a nail.

TOF measurements are usually made using the thresholding method. This involves measuring the time that it takes for the signal at the receiver to go above a threshold value after the hammer hit on the transmit probe. This technique can lead to errors if the first arrival of the signal has a low slope resulting in TOF values that vary with threshold value. The slope can vary depending on hammer hit strength and propagation distances. Also, if the threshold level is too low, noise can be detected by the threshold method instead of the first arival of the signal. Figure 6 shows a modified version of the threshold method used here to overcome these problems. TOF values and their corresponding voltage levels are obtained using the traditional threshold method for a range of threshold values. A linear fit is made for these measured TOF and signal voltage data points. The intercept of the linear fit with the time axis gives the best estimate of the actual TOF. This technique was compared to the traditional thesholding method for both same face and opposite face measurements.

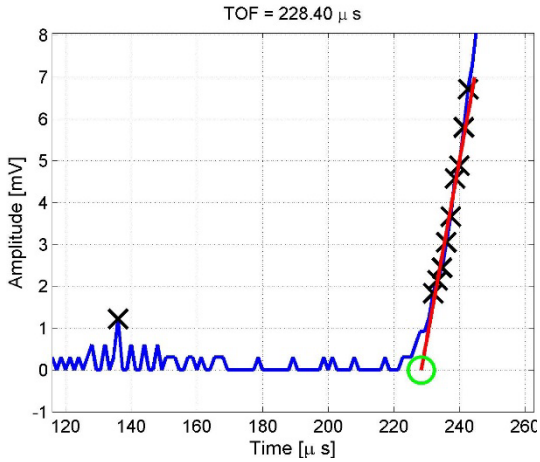

Figure 6: Diagram showing an improved method of estimating the TOF from hammer hit signal (blue line). The black crosses show where the threshold method would estimate the first arrival of the signal (TOF) for a range of threshold values. In the improved method, a linear fit (red line) is placed through the black crosses

(omitting the lowest threshold value which was identified as picking "noise") and the intercept (green circle) with the time axis is considered to be the best eastimate of the TOF.

SAME FACE MEASUREMENTS

Same face TOF measurements were obtained using the technique described above. Average velocities for each hammer hit were then calculated using another linear least square fitting method. This assumes that the TOF values T and propagation distance z may be related through

$$z = C_L \ T, \tag{4}$$

where C_L is the velocity in the longitudinal direction. This has the linear form $y = a\,x + b$ where a is the slope and b is the intercept. TOF values for each hammer hit were, therefore, plotted on the x-axis, while the corresponding distance up the tree of each transducer was plotted on the y-axis. A linear least square fit was then made for these data points, see Figure 7. Several channels were removed from the fit process since these were found to be noisy. This may have been poor coupling to the tree stem or an electrical fault. The slope of this line gives an estimate of the average longitudinal velocity. This method provides some averaging of noise. The fact that it used Time Difference of Arrival (TDA) means that it is not necessary to measure an exact time of when the hammer hit occurs on the spike.

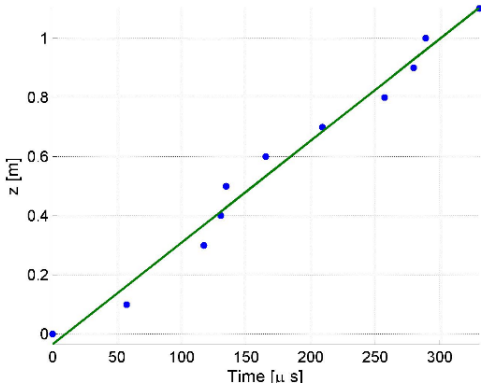

Figure 7: **Plot showing least sqares fit through same face TOF measurements for a single hammer hit. The slope (3440 m/s) gives an measurement of the mean velocity.**

The average velocity was calculted using this technique for both the standard thresholding method and the fitting method described in Figure 6. The resulting velocities are shown in Figure 8 as a function of signal amplitude, which is ideally proportional to hammer hit strength. It can be seen that the standard thresholding method gives results that vary with hammer hit strength. The new thresholding fitting method provides results that appear to vary less with hammer hit strength.

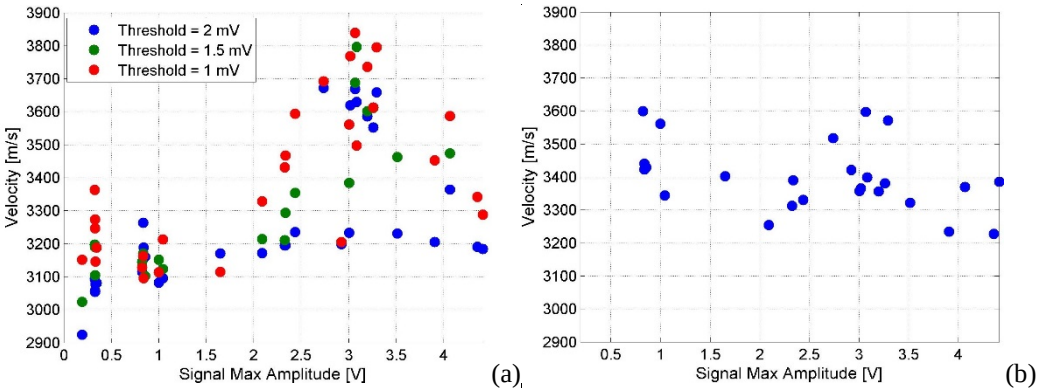

Figure 8: Plots show same face velocity measurements obtained for multiple hammer hits with a range of hammer hit strengths (and hence signal amplitude). Plot (a) shows results using the traditional thresholding method. Plot (b) shows velocity measurement obtained using the fitting technique described in Figure 6.

OPPOSITE FACE MEASUREMENTS

"Opposite face" TOF measurements were also made for the standing tree. The same transducer positions were used as for the "same face" measurement. However, hammer hits were made on a nail on the opposite face of the tree stem from the transucers. The TOF measurements were plotted as a function of distance *z*, see Figure 9(a). It can be seen that the TOF data points roughly follow a curve.

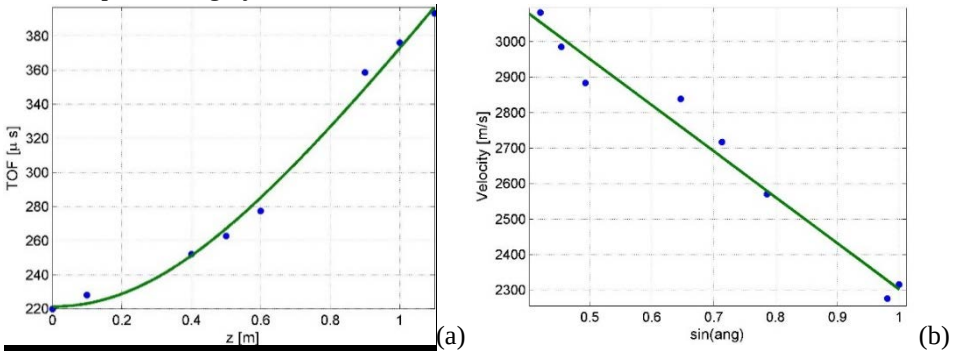

Figure 9: Example "opposite face" TOF measurement for a standing tree showing measured (a) TOF and (b) velocity data points. Overlaid are linear least squared fitted lines. For the fitted data points, the longitudinal and radial velocities were calculated as 3600 and 2300 m/s respectively.

Velocities were calculated from the measured time of flight values *T* and propagation distances *R* using

$$c_n = \frac{R_n}{T_n} = \frac{\sqrt{D^2 + z_n^2}}{T_n}. \tag{5}$$

These velocity data points formed a relatively straight line when plotted as a function of the sine of the angle

$$\sin(\theta) = \frac{D}{\sqrt{D^2 + z_n}}, \tag{6}$$

see Figure 9(b). This is similar to what had been found for previous lab measurements for a dry felled log (Legg and Bradley, 2015) and indicates that the velocity could be described as

$$c = b - a\sin(\theta), \tag{7}$$

where parameters a and b can be obtained from a least squares fit. Taking the limits as the angle goes to 0 and 90 degrees, this model suggests that the longitudinal and radial velocities can be obtained from the least squares fitted parameters using

$$c_L = b, \quad c_R = b - a. \tag{8}$$

Other models, especially one using the Kelvin-Christoffel equation should be investigated.

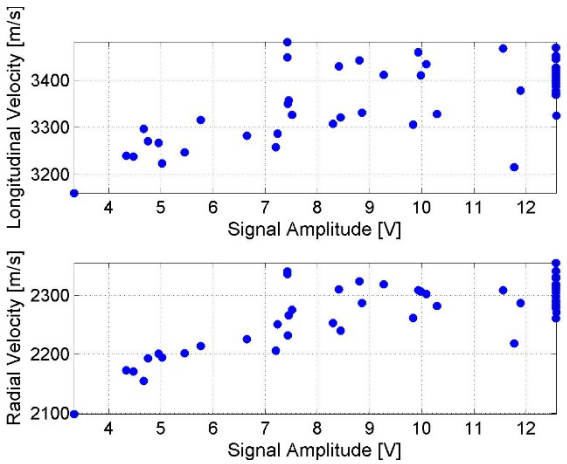

Figure 10: "Opposite face" velocity measurements obtained using the least squares fitting method.

The "opposite face" TOF velocity measurements were calculated for multiple hammer hits using the threshold fitting method described in Figure 6. These were plotted as a function of signal amplitude (and hence relative hammer hit strength). The longitudinal velocities obtained using the same and opposite face technique are similar though the opposite face measurements appear to be a bit lower. There appears to be some relationship still between hammer hit strength and velocity, particularly for the radial direction. This may indicate that there is still room for improvement in the threshold fitting technique.

CONCLUSION

There have been suggestion in some literature that time of flight measurements made on the same face of the tree tend to provide results that are biased to the outerwood stiffness. Measurements made with the receiver on the opposite face of the stem to the transmitter probe have been proposed as a potential way of obtaining stiffness measurements that are more of an average through the tree stem. However, this technique requires an anisotropic velocity model for the longitudinal-radial plane in order to extract the longitudinal velocity. This paper investigated both the "same face" and "opposite face" techniques using multiple propagation paths TOF measurements. The effect of hammer hit strength on the accuracy of threshold TOF measurements was investigated and found to be a source of error. An improved TOF extraction technique was developed that attempted to mitigate this effect. A basic model was presented that explained the "opposite face" measured data for the tree being investigated. This was used with least squares fitting to estimate the longitudinal and radial velocity. More experiments need to be made on standing trees or freshly cut logs to see if similar results are observed. These measurements need to be made using preamps and different excitation sources. Also, other models of the wave propagation through the tree stem should be investigated, such as that provided by the Kelvin-Christoffel equation.

ACKNOWLEDGMENTS

This work was performed as part of the Growing Confidence in Forestry Future project (http://gcff.nz/). Funding was provided through Scion, the New Zealand Ministry of Business, Innovation and Employment and the New Zealand Forest Growers Levy Trust. Authors would like to acknowledge John Moore, Grant Emms, and John Lee of Scion for their help and guidance.

REFERENCES

Andrews, M., 2002. Which acoustic speed. In: *Proceedings of the 13th International Symposium on Nondestructive Testing of Wood*. pp.159–165.

Bucur, V., 2006. *Acoustics of wood*. 2nd ed. New York: Springer.

Carcione, J.M., 2007a. Anisotropic elastic media. In: *Wave fields in real media: Wave propagation in anisotropic, anelastic, porous and electromagnetic media*. Oxford, Elsevier.

Chauhan, S. and Walker, J., 2006. Variations in acoustic velocity and density with age, and their interrelationships in radiata pine. *Forest Ecology and Management*, 229(1), pp.388–394.
Dickson, R., Matheson, A., Joe, B., Ilic, J. and Owen, J., 2004. Acoustic Segregation of *Pinus radiata* logs for sawmilling. *New Zealand Journal of Forestry Science*, 34(2), pp.175–189.
Dickson, R.L., Raymond, C.A., Joe, W. and Wilkinson, C.A., 2003. Segregation of *Eucalyptus dunnii* logs using acoustics. *Forest Ecology and Management*, 179(1), pp.243–251.
Dikrallah, A., Hakam, A., Kabouchi, B., Brancheriau, L., Baillères, H., Famiri, A. and Ziani, M., 2006. Experimental analysis of acoustic anisotropy of green wood by using guided waves. *Proceedings of the ESWM-COST Action E*, 35, pp.149–154.
Grabianowski, M., Manley, B. and Walker, J., 2006. Acoustic measurements on standing trees, logs and green lumber. *Wood Science and Technology*, 40(3), pp.205–216.
Harris, P., Petherick, R. and Andrews, M., 2002. Acoustic resonance tools. In: *Proceedings, 13th International Symposium on Nondestructive Testing of Wood*. pp.195–201.
Hsu, C.Y., 2003. Radiata pine wood anatomy structure and biophysical properties. PhD thesis, Forestry Department, University of Canterbury, New Zealand.
Joe, B., Dickson, R., Raymond, C., Ilic, J. and Matheson, A., 2004. Prediction of *Eucalyptus Dunnii* and *Pinus Radiata* Timber Stiffness Using Acoustics*: A Report for the RIRDC/Land and Water Australia/FWPRDC/MDBC Joint Venture Agroforestry Program*. RIRDC.
Lasserre, J.-P., Mason, E.G. and Watt, M.S., 2007. Assessing corewood acoustic velocity and modulus of elasticity with two impact based instruments in 11-year-old trees from a clonal-spacing experiment of *Pinus radiata* D. Don. *Forest Ecology and Management*, 239(1), pp.217–221.
Legg, M and S Bradley. Measurement of stiffness of standing tress using acoustic velocity measurements made through tree stems. In 19th International Nondestructive Testing and Evaluation of Wood Symposium, pages 633–640. Rio de Janeiro, Brazil, 22–25 Sep. 2015.
Li, G., Wang, X., Feng, H., Wiedenbeck, J. and Ross, R.J., 2014. Analysis of wave velocity patterns in black cherry trees and its effect on internal decay detection. *Computers and Electronics in Agriculture*, 104, pp.32–39.
Mahon, J.M., 2007. The use of acoustics for the wood quality assessment of standing *P. taeda* trees. PhD Thesis. University of Georgia.
Mahon, J.M., Jordan, L., Schimleck, L.R., Clark, A. and Daniels, R.F., 2009. A comparison of sampling methods for a standing tree acoustic device. *Southern Journal of Applied Forestry*, 33(2), pp.62–68.
Matheson, A.C., Dickson, R.L., Spencer, D.J., Joe, B. and Ilic, J., 2002. Acoustic segregation of *Pinus radiata* logs according to stiffness. *Annals of Forest Science*, 59(5-6), pp.471–477.
Maurer, H., Schubert, S.I., Bächle, F., Clauss, S., Gsell, D., Dual, J. and Niemz, P., 2006. A simple anisotropy correction procedure for acoustic wood tomography. *Holzforschung*, 60(5), pp.567–573.
Mora, C.R., Schimleck, L.R., Isik, F., Mahon, J.M., Clark, A. and Daniels, R.F., 2009. Relationships between acoustic variables and different measures of stiffness in standing *Pinus taeda* trees. *Canadian Journal of Forest Research*, 39(8), pp.1421–1429.
Ross, R.J. and Pellerin, R.F., 1994. Nondestructive testing for assessing wood members in structures. *General Technical Report FPL-GTR-70, Forest Products Laboratory, US Department of Agriculture*.
Searles, G., 2012. *Acoustic segregation and structural timber production.* PhD thesis. Edinburgh Napier University.
Su, J., Zhang, H. and Wang, X., 2009. Stress Wave Propagation on Standing Trees-Part 2. Formation of 3D Stress Wave Contour Maps. In: *Series: Conference Proceedings*.
Svilainis, L. and Motiejunas, G., 2006. Power amplifier for ultrasonic transducer excitation. *Ultragarsas*, 1(58), pp.30–36.
Wang, X., 2013. Acoustic measurements on trees and logs: a review and analysis. *Wood Science and Technology*, 47(5), pp.965–975.
Wang, X., Ross, R.J. and Carter, P., 2007. Acoustic evaluation of wood quality in standing trees. Part I. Acoustic wave behavior. *Wood and Fiber Science*, 39(1), pp.28–38.
Wang, X., Ross, R.J., McClellan, M., Barbour, R.J., Erickson, J.R., Forsman, J.W. and McGinnis, G.D., 2001. Nondestructive evaluation of standing trees with a stress wave method. *Wood and Fiber Science*, 33(4), pp.522–533.

Wang, X.R.R.J., Brashaw, B.K., Punches, J., Erickson, J.R., Forsman, J.W. and Pellerin, R.F., 2004. Diameter effect on stress-wave evaluation of modulus of elasticity of logs. *Wood and Fiber Science*, 36(3), pp.368–377.
Zhang, H., Thurber, C. and Rowe, C., 2003. Automatic P-wave arrival detection and picking with multiscale wavelet analysis for single-component recordings. *Bulletin of the Seismological Society of America*, 93(5), pp.1904–1912.
Zhang, H., Wang, X. and Ross, R.J., 2009. Stress wave propagation on standing trees: Part 1. Time-of-flight measurement and 2D stress wave contour maps. In: *16th International Symposium on NDT/NDE of Wood*. Beijing, China, pp.12–14.
Zhang, H., Wang, X. and Su, J., 2011. Experimental investigation of stress wave propagation in standing trees. *Holzforschung*, 65(5), pp.743–748.